Abstract

Contents

Chapter 2

Theoretical Background

2.1 Overview

Rayleigh-Bénard-Poiseuille (RBP) flows describe the motion of fluids confined between two infinitely extended parallel walls, heated from below and cooled from the top, driven by a pressure gradient. The RBP configuration is illustrated in figure 2.1, where $z^*, y^*, x^*, L_z, L_x, d, h$ refer to the streamwise,
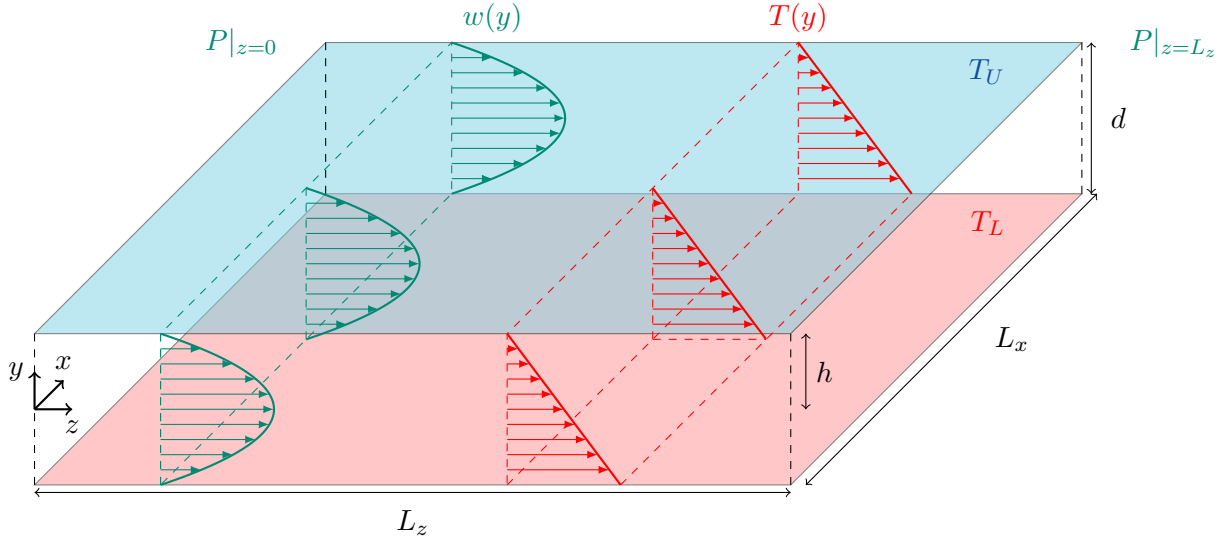
Figure 2.1: The Rayleigh-Bénard Poiseuille (RBP) flow configuration.

spanwise, wall-normal coordinates, length, span, depth and half-height of the domain respectively. We note that the asterisks*, refer to variables in dimensional form. The flow is driven by a pressure gradient along the streamwise z^* direction, $\Delta P^* = P^*|_{z^*=0} - P^*|_{z^*=L_z} < 0$, leading to the formation of a laminar Poiseuille flow, $w^*(y^*)$, for a sufficiently small ΔP. In this study, we will only consider fully-developed flow, where the boundary layer from the top and the bottom wall meets at the midplane, $y^* = 0$, and entrance effects are neglected. The RBP configuration is also unstably stratified, such that the temperature difference between the lower, T_L, and upper wall, T_U, is always positive, $\Delta T = T_L - T_U > 0$, leading to a stable linear conduction profile along the wall-normal direction, $T(y^*)$, if ΔT is kept sufficiently small.

The RBP system combines the two paradigmatic flow configurations; the classical Rayleigh-Bénard convection (RBC) and the plane Poiseuille flow (PPF), driven by buoyancy and shear forces, respectively. In the absence of a pressure gradient, the RBP configuration reduces to the classical Rayleigh-

Bénard convection problem, bringing about buoyany-driven convection for a sufficiently large unstable stratification. In the limiting case without unstable stratification, $\Delta T = 0$, the system reduces to the wall-bounded plane Poiseuille flow (PPF), where the transition towards subcritical shear-driven turbulence may be expected for a sufficiently large pressure gradient.

The onset of convection and the transition to subcritical shear-driven turbulence has been well studied independently over the past decades, however, the transitional regime where both forces interact remains largely unexplored. For instance, do buoyancy forces promote the transition to shear-driven turbulence and how does shear influence the convection? Understanding the transition to turbulence in this regime can have implications for applications such as the fabrication of thin uniform films in chemical vapour deposition [**???**] and the cooling of electronic components [**??**]. To describe the motion of the fluid in RBP configurations, we cosider non-dimensionalised Navier-Stokes equations with Boussinessq approximations,

$$\frac{\partial \mathbf{u}}{\partial t} + (\mathbf{u} \cdot \nabla)\mathbf{u} = -\nabla p + \frac{1}{Re}\nabla^2 \mathbf{u} + \frac{Ra}{Re^2 Pr}\theta, \tag{2.1a}$$

$$\frac{\partial \theta}{\partial t} + (\mathbf{u} \cdot \nabla)\theta = \frac{1}{RePr}\nabla^2 \theta, \tag{2.1b}$$

$$\nabla \cdot \mathbf{u} = 0. \tag{2.1c}$$

where $\mathbf{u}(\mathbf{x}), \theta(\mathbf{x}), p(\mathbf{x})$ refers to the nondimensionalised velocity, temperature and presure respectively. The key control parameters for RBP flows are the Rayleigh number, Ra, Reynolds number, Re, Prandlt number Pr, which are defined as follows,

$$Ra = \eta g d^3 \Delta T / \nu \kappa, \quad Re = W_c h / \nu, \quad Pr = \kappa / \nu, \quad \Gamma = L/2d, \tag{2.2}$$

where $\eta, g, \Delta T, \nu, \kappa, W_c, h, d, L$ are the thermal expansion coefficient, acceleration due to gravity, temperature difference between the bottom and top wall, kinematic viscosity, thermal diffusivity, laminar centreline velocity, domain's half-depth, full-depth, length or span respectively.

We first discuss the key developments of plane Poiseuille flow (PPF) outlining the key theoretical framework for analysing the stability of fluid flows. This is then followed by Rayleigh-Bénard convection (RBC) in §4.1.2. The historical developments involving Rayleigh-Bénard Poiseuille (RBP) flows are then expanded in §4.1.1 concluded by a section describing the hydrodynamic stability of fluid flows in §**??**

2.2 Transitional wall-bounded shear flows

Wall-bounded shear flows remain as a fundamental topic in fluid mechanics, concerning the motion of a fluid travelling in parallel to solid surfaces (such as walls), where pressence of the wall influences the flow. To satistfy the non-slip boundary conditions at the walls, the fluid layer becomes sheared, leading to velocity gradients and shear stresses within the fluid. The prototypical examples flows include the pressure-driven plane Poiseuille flow (PPF), pipe (Hagen-Poiseuille) flow, plane Couette flow and flat plate boundary layers. These geometrically simple examples enables a convenient framework amenable to the mathematical analysis of fluid motion under shear. A central question in this field is predicting the transition to turbulence, specifically, at what point does turbulence emerge as shear increases?

The earliest investigation into this transition dates back to the pipe flow experiments of **?**. In his experimental setup, the flow speed through the pipe could be controlled by regulating the inlet pressure, while injecting dye to visualise the flow, as illustrated in figure 2.2(a). At low speeds, the fluid remained laminar, whereby the fluid layers moved in smooth parallel 'laminates', resulting to a single streak of steady dye in figure 2.2(b). As the speed increased, the dye begin to exhibit irregular 'sinuous' motions interspersed with laminar regions shown in figure 2.2(c). This is now referred to as the transitional/intermittent regime, alternating between the laminar and turbulent states. Beyond a critical speed, the dye breaks down entirely into chaotic 'eddies', mixing with the surrounding fluid and discolouring the flow with dye downstream in figure 2.2(d). This regime is now identified as turbulence. Reynolds conjectured that the threshold between the laminar, transitional and turbulent regimes could be characterised by non-dimensional parameter, now known as the Reynolds number, $Re = UD/\nu$, where U is the centerline velocity in the pipe, D, the pipe diameter and ν, the kinematic viscosity. He observed that flow through the pipe remained 'stable' and laminar for $Re < 1900$, while it became 'unstable' and turbulent for $Re > 2000$ [**?**]. His remarks led to the concept of the stability of fluid flows.
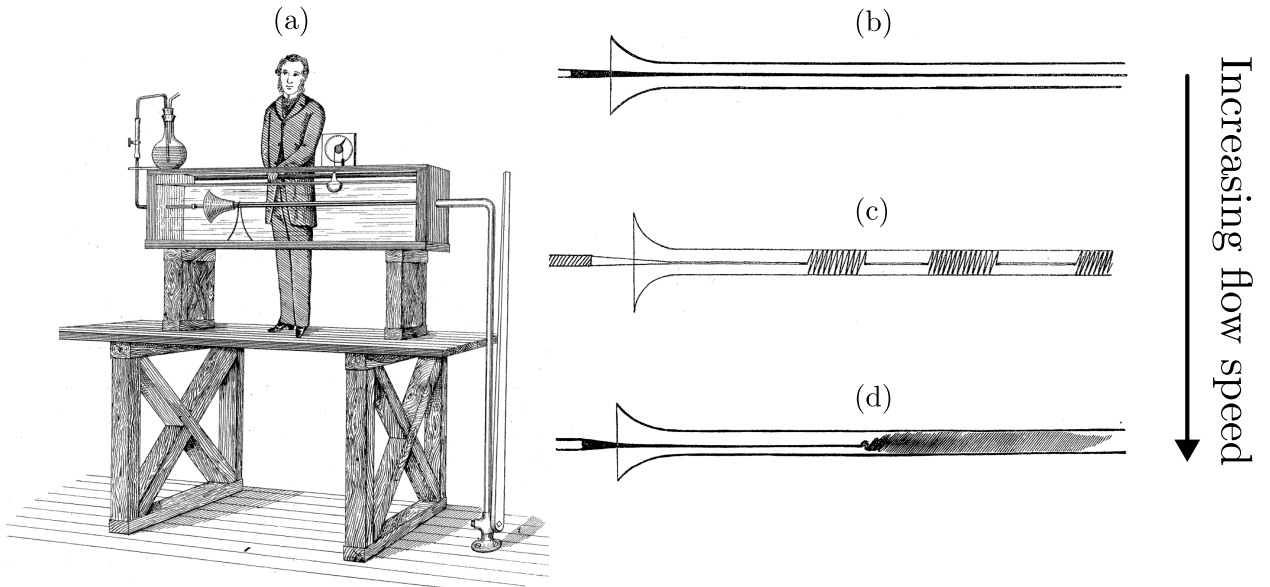
Figure 2.2: (a) Osbourne Reynolds pipe experiment with the dye injection apparatus, illustrating the (b) laminar flow, (c) intermittent regime and (d) turbulent flow as the flow speed is increased, taken from [**?**].

2.2.1 Linear Stability Analysis

Following Reynolds' experiment, interest towards the mathematical analysis of the stability of fluid flows grew in early 20st century. The typical approach begins with decomposing the velocity field, $\mathbf{u}(\mathbf{x}, t)$, into a laminar (base) state, $U(y)$ (assumed to depend only on the wall-normal direction here), and the velocity perturbations, $\mathbf{u}'(\mathbf{x}, t)$, with pressure similarly decomposed as,

$$\mathbf{u}(\mathbf{x}) = U(y) + \mathbf{u}'(\mathbf{x}, t), \quad \text{and} \quad p(\mathbf{x}, t) = P(x) + p'(\mathbf{x}, t). \tag{2.3}$$

Substituing into the Navier-Stokes equations of equation (2.1) and dropping nonlinear pertubrations terms $(\mathbf{u}' \cdot \nabla)\mathbf{u}'$, we the linearised perturbation equations,

$$\frac{\partial \mathbf{u}'}{\partial t} + (U \cdot \nabla)\mathbf{u}' + (\mathbf{u}' \cdot \nabla)U = -\nabla p' + \frac{1}{Re}\nabla^2 \mathbf{u}', \tag{2.4a}$$

$$\nabla \cdot \mathbf{u}' = 0, \tag{2.4b}$$

which describes the time evolution of the perturbations, $\mathbf{u}'$, subjected to continuity. To eliminate the pressure terms, it is covenient to transform equation (2.4) using the wall-normal perturbation velocity, v', and wall-normal vorticity, $\eta' = \partial u'/\partial z - \partial w'/\partial x$, variables and introduce a wavelike ansatz for them,

$$v'(\mathbf{x}, t) = \tilde{v}(y)e^{i(\alpha x + \beta z - \omega t)}, \quad \text{and} \quad \eta'(\mathbf{x}, t) = \tilde{\eta}(y)e^{i(\alpha x + \beta z - \omega t)}. \tag{2.5}$$

where α, β, ω denotes the streamwise and spanwise wavenumbers, and complex frequency (i.e. $\omega = \omega_r + i\omega_i$), respectively. Next, we substitute the ansatz into equation 2.4, leading to the classical Orr-Sommerfeld and Squire equations [????],

$$\left[-i\omega \begin{pmatrix} k^2 - \mathcal{D}^2 & 0 \\ 0 & 1 \end{pmatrix} + \begin{pmatrix} \mathcal{L}_{OS} & 0 \\ i\beta U' & \mathcal{L}_{SQ} \end{pmatrix}\right] \begin{pmatrix} \tilde{v} \\ \tilde{\eta} \end{pmatrix} = \mathbf{0}, \tag{2.6}$$

where $\mathcal{L}_{OS}$ and $\mathcal{L}_{SQ}$ refers to the Orr-Sommerfeld and Squire operators given as,

$$\mathcal{L}_{OS} = i\alpha U(k^2 - \mathcal{D}^2) + i\alpha U'' + \frac{1}{Re}(k^2 - \mathcal{D}^2)^2, \tag{2.7a}$$

$$\mathcal{L}_{SQ} = i\alpha U + \frac{1}{Re}(k^2 - \mathcal{D}^2). \tag{2.7b}$$

$k^2, \mathcal{D}, U', U''$ denotes the sum of squared wavenumbers, $k^2 = \alpha^2 + \beta^2$, differential operator in y, first- and second- derivative of the laminar velocity, respectively. Equation (2.6) is simply an eigenvalue problem which could be represented as,

$$\mathbf{L}\tilde{\mathbf{q}} = i\omega\mathbf{M}\tilde{\mathbf{q}} \tag{2.8}$$

where,

$$\mathbf{L} = \begin{pmatrix} \mathbf{L}_{OS} & 0 \\ i\beta U' & \mathcal{L}_{SQ} \end{pmatrix}, \quad \mathbf{M}\begin{pmatrix} k^2 - \mathcal{D}^2 & 0 \\ 0 & 1 \end{pmatrix}, \quad \tilde{\mathbf{q}} = \begin{pmatrix} \tilde{v} \\ \tilde{\eta} \end{pmatrix}. \tag{2.9}$$

and $i\omega$ refers to the eigenvalue. The aim of linear stability analysis is to determine the critical Reynolds number, Re_c, which is defined as the lowest value of Re over α and β, such that $Im[\omega] = 0$. For $Re > Re_c$, perturbations could grow exponentially, departing from the laminar state. Squire's theorem implies that for any unstable three-dimensional perturbations, $\beta \neq 0$, there exist an unstable two-dimensional perturbation, $\beta = 0$ with a lower Re_c [?]. Therefore, the unstable perturbations of wall-bounded shear flows at Re_c must be two-dimensional. The theoretical calculations was first perform by ? and ? for a flat-plate boundary layer flow, yielding a critical Reynolds number based on streamwise distance x of $Re_{x,c} = Ux_c/\nu = 520$ [?]. In their honour, the unstable two-dimensional perturbations of the Orr-Sommerfeld operator is referred to as Tollmien-Schlicting (T.S) waves. For plane Poiseuille flow [?] with a critical wavenumber of $\alpha_c = 1.02$. However, turbulence in plane Poiseuille flows have

been observed at much lower Reynolds number, $Re \sim 1000 - 2000$, contradicting the results from linear stability analysis. Likewise, the onset of turbulence appear near $Re_{x,c} \approx 5 \times 10^5$ for flat plat boundary layer. A similar result holds for the plane Couette flow [?]. Despite its limitation, linear analysis analysis succeeds in predicting the critical Rayleigh number in Rayleigh-Bénard convection. One of a major limitation of linear stability analysis considered above is that it treats each eigenmode independently, referred to as *modal* analysis. However, the interaction between decaying eigenmodes may lead to a short-term amplification of perturbations, before eventually decaying. This phenomenon is referred to as *transient growth*, and the method of analysis is referred to as *non-modal* analysis, related to the normality of the linear Orr-Sommerfeld operator [?]. To demonstrate an example of
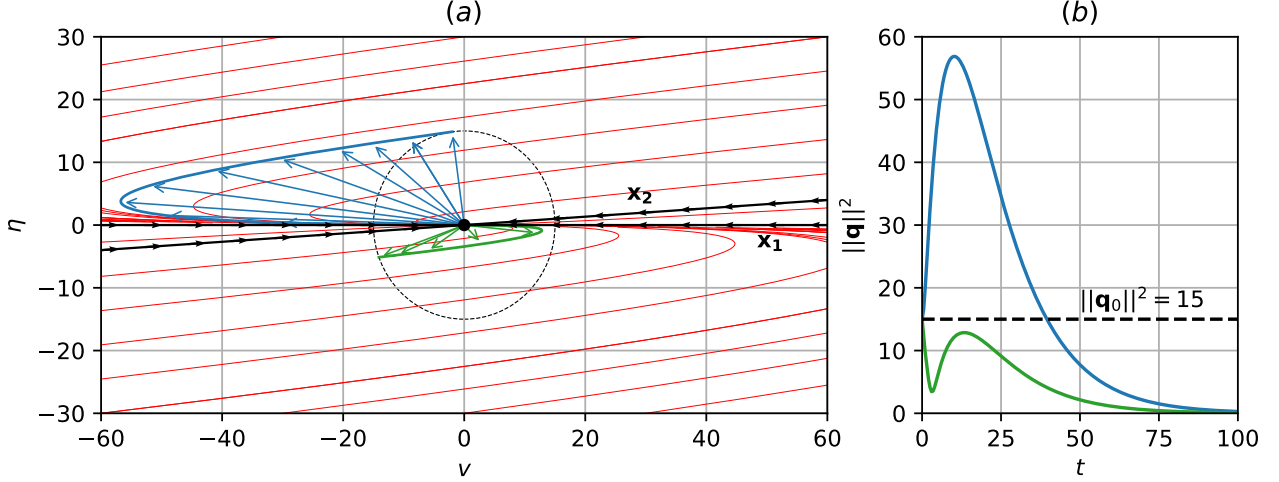

Figure 2.3: (a) The phase portrait of the toy model with $Re = 15$, (b) Transient growth.

transient growth, we consider a two-dimensional toy model governing the time-evolution of $\mathbf{q}$,

$$\frac{\mathrm{d}}{\mathrm{d}t} \begin{pmatrix} v \\ \eta \end{pmatrix} = \begin{pmatrix} -\frac{1}{Re} & -1 \\ 0 & -\frac{2}{Re} \end{pmatrix} \begin{pmatrix} v \\ \eta \end{pmatrix}, \tag{2.10}$$

where Re refers to the Reynolds number. The toy model is has negative eigenvalues, $(\lambda_1, \lambda_2) = (-1/Re, -2/Re)$, and unit eigenvectors $\mathbf{x_1} = (1,0)$, $\mathbf{x_2} = \frac{1}{\sqrt{Re^2+1}}(Re, 1)$. Judging from the negative eigenvalues, we conclude that $\mathbf{q}(t)$ will decay exponentially. However, as $Re \to \infty$, they becoming increasingly non-orthogonal approaching each other such that the angle between $\mathbf{x_1}$ and $\mathbf{x_2}$ tend towards 0. At $Re = 15$, the eigenvector pairs, $\mathbf{x_1}$ and $\mathbf{x_2}$, are highly non-orthogonal, becoming almost linear dependent shown in figure 2.3(a). For a randomly selected initial condition with an energy-norm of $||\mathbf{q_0}||_2 = 15$, where $|| \cdot ||_2$ refers to the L2-norm, the trajectory in green decays exponentially for $t \in [0, 100]$ in figure 2.3(b). In constrast, for a specifically chosen initial condition in shown as the blue trajectory, $||\mathbf{q}||_2$ is amplified nearly four times before decaying exponentially. The toy model demonstrates the significance of transient growth for a specifically chosen initial condition.

The goal of non-modal stability analysis is to searching over all initial conditions, $\tilde{\mathbf{q}}_0$, leading to the maximum amplification factor at time t, resulting in an optimisation problem,

$$G(t) = \max_{\tilde{\mathbf{q}}_0 \neq 0} \frac{\langle \tilde{\mathbf{q}}(t), \tilde{\mathbf{q}}(t) \rangle}{\langle \tilde{\mathbf{q}}_0, \tilde{\mathbf{q}}_0 \rangle}, \quad \text{s.t} \quad \langle \tilde{\mathbf{q}}_0, \tilde{\mathbf{q}}_0 \rangle = 1, \tag{2.11}$$

where, $\langle \cdot, \cdot \rangle$ refers to the inner-product defined as,

$$\langle \mathbf{x}, \mathbf{y} \rangle = \int_\Omega \mathbf{x}^H \mathbf{y} \, \mathrm{d}\Omega, \tag{2.12}$$

and $\mathbf{x}^H$ refers to the complex conjugate transpose of $\mathbf{x}$. By considering the linearised operator of (2.6), we can define a linear time-evolution given as,

$$\tilde{\mathbf{q}}(t) = \mathcal{A}(t)\tilde{\mathbf{q}}_0, \tag{2.13}$$

which takes the solution from initial conditions, $\tilde{\mathbf{q}}_0$, to $\tilde{\mathbf{q}}(t)$ at time t. Substituting the expression above into equation (2.11),

$$G(t) = \max_{\tilde{\mathbf{q}}_0 \neq 0} \frac{\langle \mathcal{A}(t)\tilde{\mathbf{q}}_0, \mathcal{A}(t)\tilde{\mathbf{q}}_0 \rangle}{\langle \tilde{\mathbf{q}}_0, \tilde{\mathbf{q}}_0 \rangle} = \langle \tilde{\mathbf{q}}_0, \mathcal{A}^\dagger(t)\mathcal{A}(t)\tilde{\mathbf{q}}_0 \rangle = \lambda_{max}(\mathcal{A}^\dagger \mathcal{A}) \tag{2.14}$$

where $\mathcal{A}^\dagger(t)$ refers to the adjoint of $\mathcal{A}(t)$. The maximum amplification factor $\max G(t)$ is the largest eigenvalue, λ_{max}, of $\mathcal{A}^\dagger \mathcal{A}$, and the eigenvalue problem is given as,

$$\mathcal{A}^\dagger(t)\mathcal{A}(t)\tilde{\mathbf{q}}_0 = \lambda \tilde{\mathbf{q}}_0, \tag{2.15}$$

where $\tilde{\mathbf{q}}_0$ refers to the eigenvector denoting the optimal initial condition. For a detailed derivation of the optimal initial conditions or forcing, the reader is referred to [??]. An alternative method of computing transient growth is computing the pseudospectral of linear operators discussed in [?], outside the scope of this thesis.

Both two-dimensional, $\beta = 0$, and three-dimensional, $\beta \neq 0$, non-modal stability analysis have been studied.

In the two-dimensional form, the optimal initial conditions are in the form of near wall vorticies tilted upstream, transiently energised referred to as the Orr-mechanism [???]. In the three-dimension form, streamwise vortices, acting as optimal initial conditions lead to the optimal response in the form of streamwise streaks [?]. Contrary to linear stability analysis which confers two-dimensional perturbations as linearly unstable, the key result in this analysis is that three-dimensional initial conditions, $\alpha = 0$, confer the optimal initial conditions leading to large transient growth at subcritical Reynolds numbers. Figure.. shows this.

2.2.2 Nonlinear dynamic systems

While the previous treats the transition process based on linear processes, turbulence is an inherent turbulent process where chaotic and quasi-periodic processes arise such as the self-sustaining process [?], arising as dynamical relationship between streaks and quasi-streamwise vortices. An alternative view of turbulence arise from the interpretation of the solution traversing through a network of unstable nonlinear solutions known as exact coherent structures (ECS) or invariant solutions [?]. Unstable nonlinear solutions were first identified by [?] in plane Couette flow. Nonlinear solutions to of plane Poiseuille flow was later identified by [?] and many others [?????].

The optimal initial conditions involve streamwise vortices which amplify streaks, related to the lift-up effect [?]. These modal and nonmodal mechanisms above highlight developments based on linear methods. It is now known that at $Re \sim 1000 - 2000$, turbulence behaves intermittently, existing as oblique bands of turbulent and laminar regions. These turbulent-laminar bands have been also

observed in shear flow systems such as Couette flow [**?**], Taylor-Couette flow [**?**], and pipe flow [**?**] (as puffs and slugs).

1. Non-modal analysis

2. Nonlinear dynamical systems

3. Spatiotemporal intermittency

Over the past decade, research efforts have been dedicated to the study of turbulent-laminar bands. The wavelengths of $24°$ oblique bands been observed to occupy $20h$ at $1900 < Re < 1400$, and $40h$ at $1300 < Re < 800$, suggesting that band widths increases as Re decrease. Between $1300 < Re < 1400$ there appears to be bistable region between bands of both band-widths [**?**]. [**??**] observed turbulent-laminar oblique bands tilted by $23.7°$ at $Re = 1430$. [**?**] computed probabilities of turbulent-laminar band splitting and decay depending on Re. As Re increases the probability of band decay decreases, while as Re decreases the probability a band splitting event decreases. By extrapolating the estimated mean lifetimes of a splitting and decay event, the crossing point (i.e equal chance of identifying a splitting and decay event after a time-scale of $t = 3 \times 10^6$) occurs at $Re_{cross} \approx 925$, in other words, Re_{cross} acts as a critical Reynolds number.

At $Re \sim 1000 - 2000$, turbulent bands can either decay spontaneously, stabilising into a laminar state, or split, forming more bands whereby turbulent-laminar bands are sustained. The probability of decay and splitting lifetimes strongly depends on the domain size and Re. At $L_z = 100h$, the critical Reynolds number of $Re_{cr} \approx 965$ have been determined statistically, whereby decay and splitting lifetimes intersect more than 10^6 advective time units. It is worth to note that for $Re < Re_{cr}$, the probably of decay is higher than splitting events, vice versa.

We seek to investigate the influence of unstable stratification quantified by Rayleigh number Ra, on the behaviour tuburlent-laminar bands. The onset of convection occurs at a critical Rayleigh number of $Ra_c > 1708$, in the form of a pair of convection rolls. When aligned in the streamwise direction, the convection rolls are seemingly analogous to a pair of counter-rotating vortices, an optimal initial condition for transient growth. Our investigation naturally answers a few questions related to turbulent-laminar bands. For example, does the onset of turbulent-laminar bands, Re_{cr} decrease with increasing Ra? Do Ra-effects influence the structure of turbulent-laminar bands i.e band angle/width?

The answers to our research will have important implications Rayleigh-Bénard Poiseuille flows, ubiquitous in atmospheric, geophysical and engineering flows. [PRESENT RBP SETUP] The governing equations of the fluid motion in given by the Navier-Stokes equations with Boussinessq approximations,

$$\frac{\partial \mathbf{u}}{\partial t} + (\mathbf{u} \cdot \nabla)\mathbf{u} = -\frac{1}{\rho}\nabla p + \nu\nabla^2\mathbf{u} + g\beta(T - T_0). \tag{2.16}$$

'

$$\frac{\partial T}{\partial t} + (\mathbf{u} \cdot \nabla)T = \kappa\nabla^2 T, \tag{2.17}$$

$$\nabla \cdot \mathbf{u} = 0. \tag{2.18}$$

with arbitrary Dirichlet and Neumann boundary conditions.

$$\mathbf{u}_d, p_d, T_d \in \Omega_d, \quad \nabla\mathbf{u}_N, p_N, T_N \in \partial\Omega_N. \tag{2.19}$$

where $\mathbf{u}, T, p$ refers to the velocity, temperature and pressure fields, primitive variables that are not known a priori and ρ, ν, κ refers to the properties of the fluid, namely, density, kinematic viscosity and thermal diffusivity. For a given set of fluid properties ρ, ν, κ and geometric properties L^*, t^*, u^* referring to an arbitrary length-, time- and velocity-scale, we are primarily interested in the behaviour of the fluid i.e if its laminar or turbulent. In other words, we have a six control parameters that describes a fluid flow of interest. To reduce the number of control parameters, we can suitably nondimensionalise the primitive variables by a velocity scale u_c, length scale, L_x, and time scale u_c/L_x, where u_c refers to the centreline velocity of a laminar flow and L_x refers to the streamwise length of the domain. The nondimensional equations with Boussienessq approximations are now given as,

$$\frac{\partial \mathbf{u}}{\partial t} + (\mathbf{u} \cdot \nabla)\mathbf{u} = -\nabla p + \frac{1}{Re}\nabla^2 \mathbf{u} + \frac{Ra}{Re^2 Pr}\theta \tag{2.20}$$

$$\frac{\partial \theta}{\partial t} + (\mathbf{u} \cdot \nabla)\theta = \frac{1}{RePr}\nabla^2 \theta, \tag{2.21}$$

$$\nabla \cdot \mathbf{u} = 0. \tag{2.22}$$

where $\mathbf{u}, \theta, p$ refers to the nondimensionalised velocity, temperature and presure. In this thesis, I am particularly focused on the transition behaviour of fluid flow driven by shear and bouyancy, addressing questions related to the onset of instabilities due to shear and buoyancy, and the (possible) competitive between shear and buoyancy driven instabilities. I would like to preface that while this thesis is dealing with onset of instabilities, it does not clearly indicate that the onset of such instabilities necessarily lead to turbulence, hence, for terminology sake, we shall be looking into transitional regimes where the fluid neither laminar nor turbulent. The main motivations are two-folds, both from an academic and applied point-of-view. Within academia, the onset and transition to turbulence in Rayleigh-Bénard Poiseuille flows remains poorly understand. Whilst there had been significant progress in our understand of transition to turbulence in independent setups, Rayleigh-Bénard convection and plane Poiseuille flows, their combined effects are not known. The thesis is structured into the follow, Chapter 1 is the introduction with literature review, chapter 2 methodology assosicated with the spectral/hp-element method, chapter 3 with results related to the the Rayleigh and Reynolds number sweep, chapter 4 with a specific focus on the bistability between spiral defect chaos and ideal straight rolls and finally chapter 5 with concluding remarks.

1. Academic motivation - flow structures, statistics, transition.

2. Application motivation - shear, heat transfer. Chip cooling, thin-film fabrication and atmospheric boundary layer.

2.3   Rayleigh-Bénard convection (RBC)

Rayleigh-Bénard convection serves as one of the paradigmatic fluid configuration for studying the dynamics of natural convection. The two basic physical mechanisms that underpins RBC is the competition between buoyancy due to heating, and resistance due to viscous forces. As the bottom plate is heated, the bottom layer fluid becomes more buoyant and tends to rise, while the colder top fluid layer is becomes relatively less buoyant and tends to sink, leading to an overturning of layers. Viscous forces between adjacent fluid parcels act to resist the motion. As buoyancy overcomes these

viscous forces, the fluid layers overturn, resulting in the initiation of convection. One of the earliest experimental work is performed by Henri Bénard [?], who observed the onset of hexagonal convection cells above a certain threshold of ΔT. To quantify the ratio between buoyancy and viscous forces, Lord Rayleigh [?] introduced the Rayleigh number, Ra, and predicted the onset of convection at a critical Rayleigh number of $Ra_c = \frac{27}{4}\pi^4 = 657.5$, with a critical wavenumber of $q_c = \frac{\pi}{\sqrt{2}d}$. His work formed the earliest record of linear stability analysis of convection.

The pioneering work from Rayleigh, and Bénard's experiment formed the early foundations of buoyancy-driven convection, now known as Rayleigh-Bénard convection. However, it is worth highlighting the key differences between Bénard's experiment and Rayleigh's analysis. In Bénard's experiments, he considered a thin layer of fluid heated which is freely exposed to ambient air, leading to the formation of hexagonal convection patterns. Unbeknownst to him at that time was that surface tension (Maragoni) effects are important in thin layers of fluid. As fluids in thin layers are being heated, surface tension decreases, generated a tangential forces towards regions of higher surface tension at the surface, where cold fluid resides, ampliying convection, now known as Bénard-Maragoni convection [?]. In Bénard's case, the effect of surface tension becomes important as the layer of fluid becomes thinner, forming hexagonal cells instead of concentric rolls in thicker layers shown by ?.

In the absence of surface tension effects, the critical Rayleigh number, Ra_c depends on the boundary condition, commonly analysed using stress-free or rigid-rigid (no-slip) boundary conditions. In Rayleigh's work, he considered a stress-free condition at the wall, $\partial u/\partial n = 0$, where analytical solutions are admittable. The critical Rayleigh number for the rigid-rigid (no-slip) case is at $Ra_c = 1707.8$ and $q_c = 3.12/d$ (or $\lambda_c \approx 2d$), computed later by ?, and is independent or Pr [?]. Notably, the size of a single convection roll in the rigid-rigid case, $l_{roll} = 1/2\lambda_c \approx d$, suggesting that the distance separating the two plates dictates the length scale of the covection roll. In this work, I will investigate RBC with no-slip velocity boundary conditions, herein referred to RBC for the rest of the thesis.

Slightly above the onset of convection, described using the reduced Rayleigh number $\varepsilon = (\frac{Ra}{Ra_c} - 1)$, a set of stable convection rolls near q_c are found to exist (CITATIONS?). The theoretical foundations of performing stability analysis using expansion in powers of amplitude (*weakly nonlinear analysis*) was considered by ?, in which he applied it to the problem of parallel shear flows. The important contribution was that slightly above the onset, stable stationary rolls are found within the range of $Ra > Ra_c + 3\eta(\alpha - \alpha_c)^2$, where $\eta = \frac{1}{2}\frac{\partial Ra}{\partial \alpha}|_{Ra_c}$. ? then extended the same technique to Rayleigh-Bénard convection, in which η was found to depend on Pr. Whilst this technique is useful in detailing the stability regions of stationary rolls, it appears to be limited as it contradict some experiments in which time-dependent oscillatory rolls were discovered [??], which has been found to be a secondary instability of stationary convection rolls with complex eigenvalues. As noted by ?, the applicability of weakly nonlinear analysis is limited to small ε. This limitation is addressed by using directly computing the linear stability of saturated convection rolls computed based on a Galerkin truncation and a root-finding algorithm. The results from linear stability analysis led to the well known Busse balloon which described the stability boundary of the convection rolls in the two dimensional space of $\varepsilon - q$, known as the Busse balloon [?] (figure 2.4).

While the Busse balloon describes the stability boundaries of ISRs over a range of wavenumbers, predicting the wavenumber of an ISR state remains an central challenge [?]. Indeed, experimental investigations of RBC in moderate domain sizes ($\Gamma \geq 7$, where Γ refers to the domain's aspect ratio) in rectangular (straight rolls) and cylinderical (concentric rolls) domains showed that the wavenumbers are confined within the Busse balloon. As ε is was continously modified, the ISRs with wavenumbers
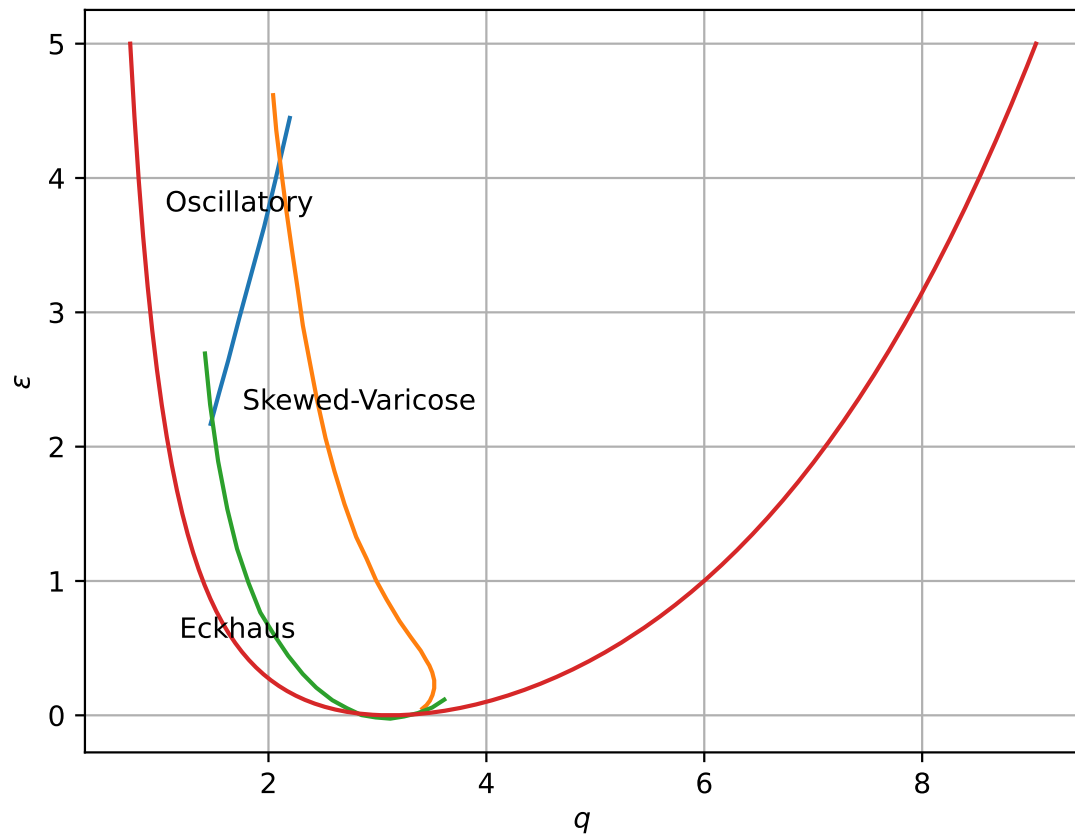
Figure 2.4: The Busse ballon describes the stability boundaries of ISRs in a $\varepsilon - q$ space. For larger wavenumbers, the instability mechanisms is described by the skewed-varicose (SV) instability. For smaller wavenumbers, the instability mechanism is described by the Eckhaus instability. For large ε, the instability is described by the onset of oscillatory instability. Busse ballon diigitised from [?] for $Pr \approx 1$

that are now outside of the Busse balloon, rolls dislocations and defects spontaneously nucleate, either increasing or decreasing the roll wavenumber, adhering to the the stability boundaries of the Busse balloon. The hysteretic nature of the system implies that the roll wavenumber of the ISRs strongly depends on the system's history [**?**].

To complicate the subject further, ISRs appear to be an exception rather than the rule [**?**] as multiple 'non-ISR' states, in the form os squares, travelling/stationary targets, giant rotating spirals and oscillatory convection patterns have been found over the years [**???????**]. For example, investigations of cylinderical RBC in small aspect-ratio revealed eight stationary statesand two oscillatory states. These findings were later supported by numerical experiments and bifurcation analyses.

1. Saturated States

2. Busse balloon for $Pr = 1$

3. Skew-varicose, Eckhaus, Cross-roll instabilities

4. Low Pr and high Pr.

5. What happens above the Busse balloon?

1. Statisitical description of spatial-temporal chaos (i.e correlation length, time etc..)

2. Challenge with quantifying the onset

2.4 Rayleigh-Bénard Poiseuille (RBP) flows

? first investigated the primary instabilities of RBP flows, which can be determined by Re, Ra, Pr, and the planar x-z perturbations wavenumbers α, β respectively. For a given Ra and Pr, the neutral stability curves are limited by the development of Tollmien-Schlicting waves for $Re \geq Re_{TS} = 5772.22$ [**?**], and convection rolls within $0 \leq Re < Re_{TS}$. Convection rolls can be categorised based on their orientation to the mean flow, namely, longitudinal ($\alpha = 0, \beta \neq 0$), transverse ($\alpha \neq 0, \beta = 0$) and oblique rolls ($\alpha \neq 0, \beta \neq 0$). The linearised system governing the onset of longitudinal rolls is analogous to the linearised RBC system, with a critical Rayleigh number, $Ra_{\parallel} = Ra_{RB} = 1708.8$ and critical wavenumber, $\alpha_{\parallel} = \alpha_{RB} = 3.13$ [**??**], independent of Re and Pr. The critical Rayleigh number for oblique and transverse rolls matches that of RBC at $Re = 0$ due to horizontal isotropy, but increases as Re increases, depending on Pr, i.e., $Ra_{\perp} = f(Re, Pr)$ [**???**]. When spatially developing instabilities are considered, longitudinal rolls are always convectively unstable, and transverse rolls can become absolutely unstable [**???**]. Nonmodal stability analyses of subcritical RBP indicate that the optimal transient growth G_{max} increases gradually with Ra. The wavenumber of the optimal initial conditions, β_{max}, resembles that observed in shear flows [**?**], and gradually approaches the critical wavenumber of convection rolls, $\alpha_{\parallel}$, as Ra increases [**?**]. For $Re > 0$, the longitudinal rolls appear as the dominant primary instability [**?**]. Secondary stability analyses of longitudinal rolls reveal a wavy instability near $Re \sim 100$ [**?**], leading to wavy longitudinal rolls, which are convectively unstable [**??**]. The influence of finite lateral extensions in RBP flows on the stability of longitudinal and transverse rolls [**??**], as well as wavy rolls [**??**], has been reported. In finite streamwise extensions of RBP flows, the onset of convection rolls and the heat flux variations due to entrance effects have been investigated [**???**]. More recently, shear-driven turbulence can enhance heat fluxes in turbulent RBP flows [**???**]. RBP

flows with sinusoidal heating and wavy walls have also been studied [**?**]. For an in-depth discussion of RBP flows, see the reviews by **?** and **?**.

Bibliography

Kerstin Avila, David Moxey, Alberto De Lozar, Marc Avila, Dwight Barkley, and Björn Hof. The Onset of Turbulence in Pipe Flow. *Science*, 333(6039):192–196, July 2011. ISSN 0036-8075, 1095-9203. doi: 10.1126/science.1203223. URL https://www.science.org/doi/10.1126/science.1203223.

Eberhard Bodenschatz, Werner Pesch, and Guenter Ahlers. Recent Developments in Rayleigh-Bénard Convection. *Annual Review of Fluid Mechanics*, 32(1):709–778, January 2000. ISSN 0066-4189, 1545-4479. doi: 10.1146/annurev.fluid.32.1.709. URL https://www.annualreviews.org/doi/10.1146/annurev.fluid.32.1.709.

Katarzyna Borońska and Laurette S. Tuckerman. Extreme multiplicity in cylindrical Rayleigh-Bénard convection. I. Time dependence and oscillations. *Physical Review E*, 81(3):036320, March 2010a. ISSN 1539-3755, 1550-2376. doi: 10.1103/PhysRevE.81.036320. URL https://link.aps.org/doi/10.1103/PhysRevE.81.036320.

Katarzyna Borońska and Laurette S. Tuckerman. Extreme multiplicity in cylindrical Rayleigh-Bénard convection. II. Bifurcation diagram and symmetry classification. *Physical Review E*, 81(3):036321, March 2010b. ISSN 1539-3755, 1550-2376. doi: 10.1103/PhysRevE.81.036321. URL https://link.aps.org/doi/10.1103/PhysRevE.81.036321.

F. H. Busse. The oscillatory instability of convection rolls in a low Prandtl number fluid. *Journal of Fluid Mechanics*, 52(1):97–112, March 1972. ISSN 0022-1120, 1469-7645. doi: 10.1017/S0022112072002988. URL https://www.cambridge.org/core/product/identifier/S0022112072002988/type/journal_article.

F H Busse. Non-linear properties of thermal convection. *Reports on Progress in Physics*, 41(12): 1929–1967, December 1978. ISSN 0034-4885, 1361-6633. doi: 10.1088/0034-4885/41/12/003. URL https://iopscience.iop.org/article/10.1088/0034-4885/41/12/003.

F. H. Busse and J. A. Whitehead. Instabilities of convection rolls in a high Prandtl number fluid. *Journal of Fluid Mechanics*, 47(2):305–320, May 1971. ISSN 0022-1120, 1469-7645. doi: 10.1017/S0022112071001071. URL https://www.cambridge.org/core/product/identifier/S0022112071001071/type/journal_article.

Kathryn M. Butler and Brian F. Farrell. Three-dimensional optimal perturbations in viscous shear flow. *Physics of Fluids A: Fluid Dynamics*, 4(8):1637–1650, August 1992. ISSN 0899-8213. doi: 10.1063/1.858386. URL https://pubs.aip.org/pof/article/4/8/1637/402702/Three-dimensional-optimal-perturbations-in-viscous.

Henri Bénard. Les tourbillons cellulaires dans une nappe liquide. - Méthodes optiques d'observation et d'enregistrement. *Journal de Physique Théorique et Appliquée*, 10(1):254–266, 1901. ISSN 0368-

3893. doi: 10.1051/jphystap:019010010025400. URL http://www.edpsciences.org/10.1051/jphystap:019010010025400.

Philippe Carrière and Peter A. Monkewitz. Convective versus absolute instability in mixed Rayleigh–Bénard–Poiseuille convection. *Journal of Fluid Mechanics*, 384:243–262, April 1999. ISSN 0022-1120, 1469-7645. doi: 10.1017/S0022112098004145. URL https://www.cambridge.org/core/product/identifier/S0022112098004145/type/journal_article.

R. M. Clever and F. H. Busse. Instabilities of longitudinal rolls in the presence of Poiseuille flow. *Journal of Fluid Mechanics*, 229(-1):517, August 1991. ISSN 0022-1120, 1469-7645. doi: 10.1017/S0022112091003142. URL http://www.journals.cambridge.org/abstract_S0022112091003142.

Vincent Croquette. Convective pattern dynamics at low Prandtl number: Part I. *Contemporary Physics*, 30(2):113–133, March 1989a. ISSN 0010-7514, 1366-5812. doi: 10.1080/00107518908225511. URL http://www.tandfonline.com/doi/abs/10.1080/00107518908225511.

Vincent Croquette. Convective pattern dynamics at low Prandtl number: Part II. *Contemporary Physics*, 30(3):153–171, May 1989b. ISSN 0010-7514, 1366-5812. doi: 10.1080/00107518908222594. URL http://www.tandfonline.com/doi/abs/10.1080/00107518908222594.

Y. Duguet, P. Schlatter, and D. S. Henningson. Formation of turbulent patterns near the onset of transition in plane Couette flow. *Journal of Fluid Mechanics*, 650:119–129, May 2010. ISSN 0022-1120, 1469-7645. doi: 10.1017/S0022112010000297. URL https://www.cambridge.org/core/product/identifier/S0022112010000297/type/journal_article.

Wiktor Eckhaus. *Studies in Non-Linear Stability Theory*, volume 6 of *Springer Tracts in Natural Philosophy*. Springer Berlin Heidelberg, Berlin, Heidelberg, 1965. ISBN 978-3-642-88319-4 978-3-642-88317-0. doi: 10.1007/978-3-642-88317-0. URL http://link.springer.com/10.1007/978-3-642-88317-0.

Greg Evans and Ralph Greif. Unsteady three-dimensional mixed convection in a heated horizontal channel with applications to chemical vapor deposition. *International Journal of Heat and Mass Transfer*, 34(8):2039–2051, August 1991. ISSN 00179310. doi: 10.1016/0017-9310(91)90215-Z. URL https://linkinghub.elsevier.com/retrieve/pii/001793109190215Z.

Brian F. Farrell. Optimal excitation of perturbations in viscous shear flow. *The Physics of Fluids*, 31(8):2093–2102, August 1988. ISSN 0031-9171. doi: 10.1063/1.866609. URL https://pubs.aip.org/pfl/article/31/8/2093/966463/Optimal-excitation-of-perturbations-in-viscous.

Fatin Bazilah Fauzi, Edhuan Ismail, Mohd Hanafi Ani, Syed Noh Syed Abu Bakar, Mohd Ambri Mohamed, Burhanuddin Yeop Majlis, Muhamad Faiz Md Din, and Mohd Asyadi Azam Mohd Abid. A critical review of the effects of fluid dynamics on graphene growth in atmospheric pressure chemical vapor deposition. *Journal of Materials Research*, 33(9):1088–1108, May 2018. ISSN 0884-2914, 2044-5326. doi: 10.1557/jmr.2018.39. URL http://link.springer.com/10.1557/jmr.2018.39.

K. S. Gage and W. H. Reid. The stability of thermally stratified plane Poiseuille flow. *Journal of Fluid Mechanics*, 33(1):21–32, July 1968. ISSN 0022-1120, 1469-7645. doi: 10.1017/S0022112068002326. URL https://www.cambridge.org/core/product/identifier/S0022112068002326/type/journal_article.

Sébastien Gomé, Laurette S. Tuckerman, and Dwight Barkley. Statistical transition to turbulence in plane channel flow. *Physical Review Fluids*, 5(8):083905, August 2020. ISSN 2469-990X. doi: 10.1103/PhysRevFluids.5.083905. URL https://link.aps.org/doi/10.1103/PhysRevFluids.5.083905.

Michael D. Graham and Daniel Floryan. Exact Coherent States and the Nonlinear Dynamics of Wall-Bounded Turbulent Flows. *Annual Review of Fluid Mechanics*, 53(1):227–253, January 2021. ISSN 0066-4189, 1545-4479. doi: 10.1146/annurev-fluid-051820-020223. URL https://www.annualreviews.org/doi/10.1146/annurev-fluid-051820-020223.

James M. Hamilton, John Kim, and Fabian Waleffe. Regeneration mechanisms of near-wall turbulence structures. *Journal of Fluid Mechanics*, 287:317–348, March 1995. ISSN 0022-1120, 1469-7645. doi: 10.1017/S0022112095000978. URL https://www.cambridge.org/core/product/identifier/S0022112095000978/type/journal_article.

C.Q Hoard, C.R Robertson, and A Acrivos. Experiments on the cellular structure in bénard convection. *International Journal of Heat and Mass Transfer*, 13(5):849–856, May 1970. ISSN 00179310. doi: 10.1016/0017-9310(70)90130-4. URL https://linkinghub.elsevier.com/retrieve/pii/0017931070901304.

B. Hof, P. G. J. Lucas, and T. Mullin. Flow state multiplicity in convection. *Physics of Fluids*, 11 (10):2815–2817, October 1999. ISSN 1070-6631, 1089-7666. doi: 10.1063/1.870178. URL https://pubs.aip.org/pof/article/11/10/2815/254396/Flow-state-multiplicity-in-convection.

Mohammad Z. Hossain, Chris D. Cantwell, and Spencer J. Sherwin. A spectral/ *hp* element method for thermal convection. *International Journal for Numerical Methods in Fluids*, 93(7):2380–2395, July 2021. ISSN 0271-2091, 1097-0363. doi: 10.1002/fld.4978. URL https://onlinelibrary.wiley.com/doi/10.1002/fld.4978.

Klavs F. Jensen, Erik O. Einset, and Dimitrios I. Fotiadis. Flow Phenomena in Chemical Vapor Deposition of Thin Films. *Annual Review of Fluid Mechanics*, 23(1):197–232, January 1991. ISSN 0066-4189, 1545-4479. doi: 10.1146/annurev.fl.23.010191.001213. URL https://www.annualreviews.org/doi/10.1146/annurev.fl.23.010191.001213.

J. John Soundar Jerome, Jean-Marc Chomaz, and Patrick Huerre. Transient growth in Rayleigh-Bénard-Poiseuille/Couette convection. *Physics of Fluids*, 24(4):044103, April 2012. ISSN 1070-6631, 1089-7666. doi: 10.1063/1.4704642. URL https://pubs.aip.org/pof/article/24/4/044103/257562/Transient-growth-in-Rayleigh-Benard-Poiseuille.

Yuki Kato and Kaoru Fujimura. Prediction of pattern selection due to an interaction between longitudinal rolls and transverse modes in a flow through a rectangular channel heated from below. *Physical Review E*, 62(1):601–611, July 2000. ISSN 1063-651X, 1095-3787. doi: 10.1103/PhysRevE.62.601. URL https://link.aps.org/doi/10.1103/PhysRevE.62.601.

R.E. Kelly. The Onset and Development of Thermal Convection in Fully Developed Shear Flows. In *Advances in Applied Mechanics*, volume 31, pages 35–112. Elsevier, 1994. ISBN 978-0-12-002031-7. doi: 10.1016/S0065-2156(08)70255-2. URL https://linkinghub.elsevier.com/retrieve/pii/S0065215608702552.

K.J. Kennedy and A. Zebib. Combined free and forced convection between horizontal parallel planes: some case studies. *International Journal of Heat and Mass Transfer*, 26(3):471–474, March 1983. ISSN 00179310. doi: 10.1016/0017-9310(83)90052-2. URL https://linkinghub.elsevier.com/retrieve/pii/0017931083900522.

F.S. Lee and G.J. Hwang. The effect of asymmetric heating on the onset of thermal instability in the thermal entrance region of a parallel plate channel. *International Journal of Heat and Mass Transfer*, 34(9):2207–2218, September 1991. ISSN 00179310. doi: 10.1016/0017-9310(91)90047-I. URL https://linkinghub.elsevier.com/retrieve/pii/001793109190047I.

H. V. Mahaney, F. P. Incropera, and S. Ramadhyani. EFFECT OF WALL HEAT FLUX DISTRIBUTION ON LAMINAR MIXED CONVECTION IN THE ENTRANCE REGION OF A HORIZONTAL RECTANGULAR DUCT. *Numerical Heat Transfer*, 13(4):427–450, June 1988. ISSN 0149-5720. doi: 10.1080/10407788808913624. URL http://www.tandfonline.com/doi/abs/10.1080/10407788808913624.

Paul Manneville. Rayleigh-Bénard Convection: Thirty Years of Experimental, Theoretical, and Modeling Work. In Gerhard Höhler, Johann H. Kühn, Thomas Müller, Joachim Trümper, Andrei Ruckenstein, Peter Wölfle, Frank Steiner, Innocent Mutabazi, José Eduardo Wesfreid, and Etienne Guyon, editors, *Dynamics of Spatio-Temporal Cellular Structures*, volume 207, pages 41–65. Springer New York, New York, NY, 2006. ISBN 978-0-387-40098-3 978-0-387-25111-0. doi: 10.1007/978-0-387-25111-0_3. URL http://link.springer.com/10.1007/978-0-387-25111-0_3. Series Title: Springer Tracts in Modern Physics.

Á. Meseguer and L.N. Trefethen. Linearized pipe flow to Reynolds number 107. *Journal of Computational Physics*, 186(1):178–197, March 2003. ISSN 00219991. doi: 10.1016/S0021-9991(03)00029-9. URL https://linkinghub.elsevier.com/retrieve/pii/S0021999103000299.

H. W Müller, M Lücke, and M Kamps. Convective Patterns in Horizontal Flow. *Europhysics Letters (EPL)*, 10(5):451–456, November 1989. ISSN 0295-5075, 1286-4854. doi: 10.1209/0295-5075/10/5/011. URL https://iopscience.iop.org/article/10.1209/0295-5075/10/5/011.

H. W. Müller, M. Lücke, and M. Kamps. Transversal convection patterns in horizontal shear flow. *Physical Review A*, 45(6):3714–3726, March 1992. ISSN 1050-2947, 1094-1622. doi: 10.1103/PhysRevA.45.3714. URL https://link.aps.org/doi/10.1103/PhysRevA.45.3714.

M. Nagata. Three-dimensional finite-amplitude solutions in plane Couette flow: bifurcation from infinity. *Journal of Fluid Mechanics*, 217:519–527, August 1990. ISSN 0022-1120, 1469-7645. doi: 10.1017/S0022112090000829. URL https://www.cambridge.org/core/product/identifier/S0022112090000829/type/journal_article.

M. Nagata and K. Deguchi. Mirror-symmetric exact coherent states in plane Poiseuille flow. *Journal of Fluid Mechanics*, 735:R4, November 2013. ISSN 0022-1120, 1469-7645. doi: 10.1017/jfm.2013.515. URL https://www.cambridge.org/core/product/identifier/S0022112013005156/type/journal_article.

X. Nicolas, A. Mojtabi, and J. K. Platten. Two-dimensional numerical analysis of the Poiseuille–Bénard flow in a rectangular channel heated from below. *Physics of Fluids*, 9(2):337–348,

February 1997. ISSN 1070-6631, 1089-7666. doi: 10.1063/1.869235. URL https://pubs.aip.org/pof/article/9/2/337/259822/Two-dimensional-numerical-analysis-of-the.

X. Nicolas, J.-M. Luijkx, and J.-K. Platten. Linear stability of mixed convection flows in horizontal rectangular channels of finite transversal extension heated from below. *International Journal of Heat and Mass Transfer*, 43(4):589–610, February 2000. ISSN 00179310. doi: 10.1016/S0017-9310(99)00099-X. URL https://linkinghub.elsevier.com/retrieve/pii/S001793109900099X.

Xavier Nicolas. Revue bibliographique sur les écoulements de Poiseuille–Rayleigh–Bénard : écoulements de convection mixte en conduites rectangulaires horizontales chauffées par le bas. *International Journal of Thermal Sciences*, 41(10):961–1016, October 2002. ISSN 12900729. doi: 10.1016/S1290-0729(02)01374-1. URL https://linkinghub.elsevier.com/retrieve/pii/S1290072902013741.

Xavier Nicolas, Shihe Xin, and Noussaiba Zoueidi. Characterisation of a Wavy Convective Instability in Poiseuille-Rayleigh-Be´nard Flows: Linear Stability Analysis and Non Linear Numerical Simulations Under Random Excitations. In *2010 14th International Heat Transfer Conference, Volume 7*, pages 203–208, Washington, DC, USA, January 2010. ASMEDC. ISBN 978-0-7918-4942-2 978-0-7918-3879-2. doi: 10.1115/IHTC14-22256. URL https://asmedigitalcollection.asme.org/IHTC/proceedings/IHTC14/49422/203/360332.

C. Nonino and S. Del Giudice. Laminar mixed convection in the entrance region of horizontal rectangular ducts. *International Journal for Numerical Methods in Fluids*, 13(1):33–48, June 1991. ISSN 0271-2091, 1097-0363. doi: 10.1002/fld.1650130103. URL https://onlinelibrary.wiley.com/doi/10.1002/fld.1650130103.

William M'F. Orr. The Stability or Instability of the Steady Motions of a Perfect Liquid and of a Viscous Liquid. Part II: A Viscous Liquid. *Proceedings of the Royal Irish Academy. Section A: Mathematical and Physical Sciences*, 27:69–138, 1907. ISSN 00358975. URL http://www.jstor.org/stable/20490591. Publisher: Royal Irish Academy.

Steven A. Orszag. Accurate solution of the Orr–Sommerfeld stability equation. *Journal of Fluid Mechanics*, 50(4):689–703, December 1971. ISSN 0022-1120, 1469-7645. doi: 10.1017/S0022112071002842. URL https://www.cambridge.org/core/product/identifier/S0022112071002842/type/journal_article.

Hervé Pabiou, Sophie Mergui, and Christine Bénard. Wavy secondary instability of longitudinal rolls in RayleighPoiseuille flows. *Journal of Fluid Mechanics*, 542(-1):175, October 2005. ISSN 0022-1120, 1469-7645. doi: 10.1017/S0022112005006154. URL http://www.journals.cambridge.org/abstract_S0022112005006154.

Anne Pellew and Richard Vynne Southwell. On maintained convective motion in a fluid heated from below. *Proceedings of the Royal Society of London. Series A. Mathematical and Physical Sciences*, 176(966):312–343, November 1940. ISSN 0080-4630, 2053-9169. doi: 10.1098/rspa.1940.0092. URL https://royalsocietypublishing.org/doi/10.1098/rspa.1940.0092.

Sergio Pirozzoli, Matteo Bernardini, Roberto Verzicco, and Paolo Orlandi. Mixed convection in turbulent channels with unstable stratification. *Journal of Fluid Mechanics*, 821:482–516, June 2017.

ISSN 0022-1120, 1469-7645. doi: 10.1017/jfm.2017.216. URL https://www.cambridge.org/core/product/identifier/S0022112017002166/type/journal_article.

Brendan B. Plapp, David A. Egolf, Eberhard Bodenschatz, and Werner Pesch. Dynamics and Selection of Giant Spirals in Rayleigh-Bénard Convection. *Physical Review Letters*, 81(24):5334–5337, December 1998. ISSN 0031-9007, 1079-7114. doi: 10.1103/PhysRevLett.81.5334. URL https://link.aps.org/doi/10.1103/PhysRevLett.81.5334.

Arnaud Prigent, Guillaume Grégoire, Hugues Chaté, and Olivier Dauchot. Long-wavelength modulation of turbulent shear flows. *Physica D: Nonlinear Phenomena*, 174(1-4):100–113, January 2003. ISSN 01672789. doi: 10.1016/S0167-2789(02)00685-1. URL https://linkinghub.elsevier.com/retrieve/pii/S0167278902006851.

Subhashis Ray and J. Srinivasan. Analysis of conjugate laminar mixed convection cooling in a shrouded array of electronic components. *International Journal of Heat and Mass Transfer*, 35(4):815–822, April 1992. ISSN 00179310. doi: 10.1016/0017-9310(92)90249-R. URL https://linkinghub.elsevier.com/retrieve/pii/001793109290249R.

Lord Rayleigh. LIX. *On convection currents in a horizontal layer of fluid, when the higher temperature is on the under side. The London, Edinburgh, and Dublin Philosophical Magazine and Journal of Science*, 32(192):529–546, December 1916. ISSN 1941-5982, 1941-5990. doi: 10.1080/14786441608635602. URL https://www.tandfonline.com/doi/full/10.1080/14786441608635602.

Satish C. Reddy and Dan S. Henningson. Energy growth in viscous channel flows. *Journal of Fluid Mechanics*, 252:209–238, July 1993. ISSN 0022-1120, 1469-7645. doi: 10.1017/S0022112093003738. URL https://www.cambridge.org/core/product/identifier/S0022112093003738/type/journal_article.

Satish C. Reddy, Peter J. Schmid, and Dan S. Henningson. Pseudospectra of the Orr–Sommerfeld Operator. *SIAM Journal on Applied Mathematics*, 53(1):15–47, February 1993. ISSN 0036-1399, 1095-712X. doi: 10.1137/0153002. URL http://epubs.siam.org/doi/10.1137/0153002.

Osborne Reynolds. XXIX. An experimental investigation of the circumstances which determine whether the motion of water shall be direct or sinuous, and of the law of resistance in parallel channels. *Philosophical Transactions of the Royal Society of London*, 174:935–982, December 1883. ISSN 0261-0523, 2053-9223. doi: 10.1098/rstl.1883.0029. URL https://royalsocietypublishing.org/doi/10.1098/rstl.1883.0029.

Osborne Reynolds. IV. On the dynamical theory of incompressible viscous fluids and the determination of the criterion. *Philosophical Transactions of the Royal Society of London. (A.)*, 186:123–164, December 1895. ISSN 0264-3820, 2053-9231. doi: 10.1098/rsta.1895.0004. URL https://royalsocietypublishing.org/doi/10.1098/rsta.1895.0004.

H. T. Rossby. A study of Bénard convection with and without rotation. *Journal of Fluid Mechanics*, 36(2):309–335, April 1969. ISSN 0022-1120, 1469-7645. doi: 10.1017/S0022112069001674. URL https://www.cambridge.org/core/product/identifier/S0022112069001674/type/journal_article.

Sten Rüdiger and Fred Feudel. Pattern formation in Rayleigh-Bénard convection in a cylindrical container. *Physical Review E*, 62(4):4927–4931, October 2000. ISSN 1063-651X, 1095-3787. doi: 10.1103/PhysRevE.62.4927. URL https://link.aps.org/doi/10.1103/PhysRevE.62.4927.

A. Scagliarini, H. Einarsson, Á. Gylfason, and F. Toschi. Law of the wall in an unstably stratified turbulent channel flow. *Journal of Fluid Mechanics*, 781:R5, October 2015. ISSN 0022-1120, 1469-7645. doi: 10.1017/jfm.2015.498. URL https://www.cambridge.org/core/product/identifier/S002211201500498X/type/journal_article.

Andrea Scagliarini, Armann Gylfason, and Federico Toschi. Heat flux scaling in turbulent Rayleigh-Bénard convection with an imposed longitudinal wind. *Physical Review E*, 89(4):043012, April 2014. ISSN 1539-3755, 1550-2376. doi: 10.1103/PhysRevE.89.043012. URL http://arxiv.org/abs/1311.4598. arXiv:1311.4598 [physics].

H. Schlichting. Zur Enstehung der Turbulenz bei der Plattenströmung. *Nachrichten von der Gesellschaft der Wissenschaften zu Göttingen, Mathematisch-Physikalische Klasse*, 1933:181–208, 1933. URL http://eudml.org/doc/59420.

Hermann Schlichting and Klaus Gersten. Onset of Turbulence (Stability Theory). In *Boundary-Layer Theory*, pages 415–496. Springer Berlin Heidelberg, Berlin, Heidelberg, 2017. ISBN 978-3-662-52917-1 978-3-662-52919-5. doi: 10.1007/978-3-662-52919-5_15. URL http://link.springer.com/10.1007/978-3-662-52919-5_15.

Peter J. Schmid. Nonmodal Stability Theory. *Annual Review of Fluid Mechanics*, 39(1):129–162, January 2007. ISSN 0066-4189, 1545-4479. doi: 10.1146/annurev.fluid.38.050304.092139. URL https://www.annualreviews.org/doi/10.1146/annurev.fluid.38.050304.092139.

Peter J. Schmid and Dan S. Henningson. *Stability and Transition in Shear Flows*, volume 142 of *Applied Mathematical Sciences*. Springer New York, New York, NY, 2001. ISBN 978-1-4612-6564-1 978-1-4613-0185-1. doi: 10.1007/978-1-4613-0185-1. URL http://link.springer.com/10.1007/978-1-4613-0185-1.

Arnold Sommerfeld. *Ein beitrag zur hydrodynamischen erklaerung der turbulenten fluessigkeitsbewegungen*. 1909.

Herbert Brian Squire. On the stability for three-dimensional disturbances of viscous fluid flow between parallel walls. *Proceedings of the Royal Society of London. Series A, Containing Papers of a Mathematical and Physical Character*, 142(847):621–628, November 1933. ISSN 0950-1207, 2053-9150. doi: 10.1098/rspa.1933.0193. URL https://royalsocietypublishing.org/doi/10.1098/rspa.1933.0193.

Sadayoshi Toh and Tomoaki Itano. A periodic-like solution in channel flow. *Journal of Fluid Mechanics*, 481:67–76, April 2003. ISSN 00221120, 14697645. doi: 10.1017/S0022112003003768. URL http://www.journals.cambridge.org/abstract_S0022112003003768.

W. Tollmien. Über die Entstehung der Turbulenz. 1. Mitteilung. *Nachrichten von der Gesellschaft der Wissenschaften zu Göttingen, Mathematisch-Physikalische Klasse*, 1929:21–44, 1928. URL http://eudml.org/doc/59276.

Lloyd N. Trefethen. Pseudospectra of Linear Operators. *SIAM Review*, 39(3):383–406, January 1997. ISSN 0036-1445, 1095-7200. doi: 10.1137/S0036144595295284. URL http://epubs.siam.org/doi/10.1137/S0036144595295284.

Takahiro Tsukahara, Kaoru Iwamoto, Hiroshi Kawamura, and Tetsuaki Takeda. DNS of heat transfer in a transitional channel flow accompanied by a turbulent puff-like structure, September 2014a. URL http://arxiv.org/abs/1406.0586. arXiv:1406.0586 [physics].

Takahiro Tsukahara, Yohji Seki, Hiroshi Kawamura, and Daisuke Tochio. DNS of turbulent channel flow at very low Reynolds numbers, September 2014b. URL http://arxiv.org/abs/1406.0248. arXiv:1406.0248 [physics].

Laurette S. Tuckerman, Tobias Kreilos, Hecke Schrobsdorff, Tobias M. Schneider, and John F. Gibson. Turbulent-laminar patterns in plane Poiseuille flow. *Physics of Fluids*, 26(11):114103, November 2014. ISSN 1070-6631, 1089-7666. doi: 10.1063/1.4900874. URL https://pubs.aip.org/pof/article/26/11/114103/315350/Turbulent-laminar-patterns-in-plane-Poiseuille.

Fabian Waleffe. Exact coherent structures in channel flow. *Journal of Fluid Mechanics*, 435:93–102, May 2001. ISSN 0022-1120, 1469-7645. doi: 10.1017/S0022112001004189. URL https://www.cambridge.org/core/product/identifier/S0022112001004189/type/journal_article.

Fabian Waleffe. Homotopy of exact coherent structures in plane shear flows. *Physics of Fluids*, 15(6):1517–1534, June 2003. ISSN 1070-6631, 1089-7666. doi: 10.1063/1.1566753. URL https://pubs.aip.org/pof/article/15/6/1517/448391/Homotopy-of-exact-coherent-structures-in-plane.

D. P. Wall and M. Nagata. Exact coherent states in channel flow. *Journal of Fluid Mechanics*, 788:444–468, February 2016. ISSN 0022-1120, 1469-7645. doi: 10.1017/jfm.2015.685. URL https://www.cambridge.org/core/product/identifier/S0022112015006850/type/journal_article.

G. E. Willis and J. W. Deardorff. The oscillatory motions of Rayleigh convection. *Journal of Fluid Mechanics*, 44(04):661, December 1970. ISSN 0022-1120, 1469-7645. doi: 10.1017/S0022112070002070. URL http://www.journals.cambridge.org/abstract_S0022112070002070.

Shihe Xin, Xavier Nicolas, and Patrick Le Quéré. Stability analyses of Longitudinal Rolls of Poiseuille-Rayleigh-Bénard Flows in Air-Filled Channels of Finite Transversal Extension. *Numerical Heat Transfer, Part A: Applications*, 50(5):467–490, July 2006. ISSN 1040-7782, 1521-0634. doi: 10.1080/10407780600620079. URL http://www.tandfonline.com/doi/abs/10.1080/10407780600620079.